CHAPTER I

LITERATURE SURVEY

1.1. Background

The IFCON® process (U.S. Patents 5411570, 6146437, 6537342) is a direct steelmaking process reacting iron ore fines, coal and fluxes in a single vessel to produce crude liquid steel of ~0.1%C. The furnace cross section is shown diagrammatically in **Fig. 1**, and indicates the three main phase volumes: freeboard, heaps, and metal bath. The material mixture of ore fines, coal and fluxes of -10 mm is fed onto the liquid metal bath to form heaps floating on the metal bath. The freeboard is heated by combustion of natural gas and an air and oxygen blast blown into the freeboard via burners. In addition to the natural gas combusted in the freeboard, coal volatiles and reduction product gas from the heaps are combusted to generate heat in the freeboard, which in turn heats the heap surface. This upper section of the heap, where solid state reduction takes place, is heated by fossil fuel energy. Solid state reduction of the iron ore takes place at the heap surface, within the top 20-25 mm layer of material mixture. The material at the heap surface can be heated to temperatures the order of 1400°C, or higher, provided the furnace refractories are not damaged and the iron product remains in the solid state to be melted at the interface between the heap bottom and the metal bath.

Fig. 1: IFCON® furnace cross section

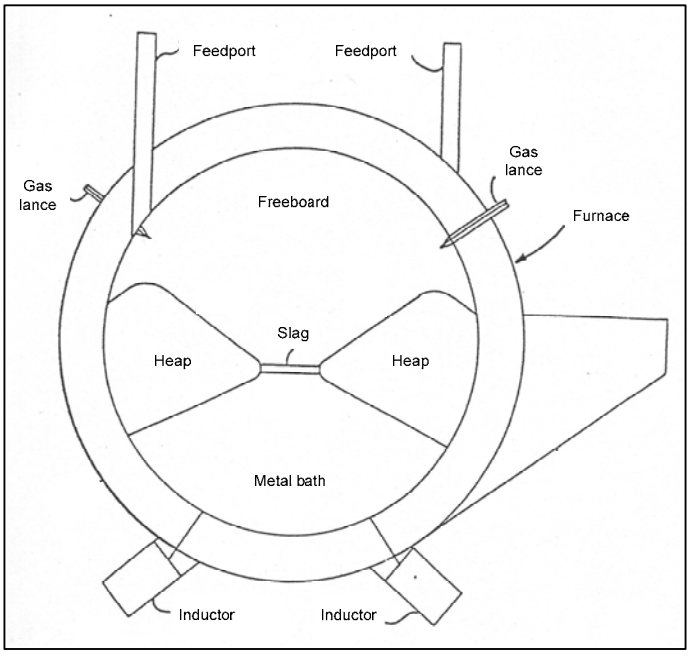

The bottom portions of the heaps are heated from the metal bath, which is in turn heated by inductors. The energy input to the metal bath is regulated to maintain the desired metal bath temperature whilst providing sufficient energy for final reduction and melting of the heaps into metal and slag. For steel production the metal bath is operated 50°C to 100°C above the liquidus temperature of the steel.

It is important to quantify and understand ore reduction extent, coal devolatlisation and carbon consumption occurring simultaneously at the heap surface. The carbon content of metallised product formed at the heap surface is also important in development of process understanding because the aim is to make crude steel, not hot metal.

1.2. Iron Ore Reduction with Coal/Carbon

The reduction of iron oxide with carbon is endothermic. For this reason, heat transfer to a mixture of iron oxide and carbon is essential, and in many cases temperature differences can arise within the mixture of solids. In some studies the intention was for a non-isothermal experiment in order to simulate reaction conditions specific to a process e.g. Dutta and Gosh (1994), Wang *et al.* (1997, 1998) and Fortini and Fruehan (2005) reacted composite pellets to simulate conditions in industrial rotary hearth furnace reactors such as Inmetco (Gou and Lu, 1998) and Fastmet (Hoffman and Harada, 1997). Mookherjee *et al.* (1985b) reacted a core of iron ore, surrounded by a cylinder of coal char, non-isothermally to simulate reaction conditions in the Hoganas process in which the oxide and coal are not mixed. Abraham and Gosh (1979) used an experimental set-up in which the electrode graphite powder and the hematite pellet were contained in the same crucible, but physically separated at various distances. The aim was to simulate reaction conditions in the rotary kiln process. Prakash (1994), Prakash and Ray (1990, 1991) and Prakash *et al.* (1986) reacted a mixed bed of coal and ore in the MBR (Moving Bed Reactor) to simulate a vertical retort process for DRI (Directly Reduced Iron) production. Shivaramakrishna *et al.* (1996) reacted coal-ore composite pellets with external coal in an electrically heated rotary tube furnace to simulate DRI production in a rotary kiln furnace. Roman-Moguel and Brimacombe (1988) used a bench scale batch rotary kiln to study the use of unagglomerated iron ore as feed material.

In many cases, it appear that experiments performed on mixtures of carbon/coal and iron ore were intended to yield isothermal reactions, but in most instances the experiment turned out to be non-isothermal because of relatively large sample sizes and/or sample containment arrangements which hampered heat transfer. This unintended outcome is usually ignored and the experimental results are reported as isothermal, and usually the furnace temperature is taken as the experimental temperature.

Isothermal reaction is only obtained when small masses of material, of the order of one gram, is used-as in the work of Otsuka and Kunii (1969), Rao (1971), Fruehan (1977) and Mookherjee *et al.*

(1985a). Even in a relatively small mixed bed sample the difference between the furnace temperature and the material mixture can be significant as shown by Haque *et al*. (1993) for reaction of –2 +1 mm iron ore – coal mixture at furnace temperatures of 900-1050°C in a mild steel crucible of 30 mm diameter and 50 mm height for 100-200 minutes total reaction time. The sample temperature reached the furnace temperature after 19-22 minutes of heating time. Mookherjee *et al.* (1986) reacted 45 g samples of coal and ore arranged as separate cylindrical shapes in mild steel crucibles, of 33 mm i.d. and 50 mm height, at furnace temperatures of 850 to 1050°C. The sample temperature was measured, starting when the sample was introduced into the furnace. The sample temperature reached the furnace temperature after 20-30 minutes reaction time. The total reaction time was 150-180 minutes.

Seaton *et al*. (1983) showed that the heating conditions were non-isothermal in 14 mm diameter magnetite and hematite containing composite pellets. In magnetite composite pellets the measured temperature profiles at the pellet centre and pellet surface showed that these two temperatures equalised after 10, 15, and 27 minutes at furnace temperatures of 1200°C, 1000°C and 1100°C, when reduction was complete or ceased. According to Seaton *et al*. (1983) the maximum temperature differential between the pellet centre and pellet surface occurs when the gasification (Boudouard) reaction is predominant. The surface temperatures reached values close to the furnace temperature after 7.5, 16 and 4 minutes for furnace temperatures of 1200°C, 1000°C and 1100°C, respectively. Seaton *et al*. (1983) calculated apparent activation energies, but also did heat transfer calculations for one experiment to show the importance of heat transfer. The heat transfer calculations showed that heat flux to the sample surface becomes insufficient to drive the gasification reaction in the latter part of the reaction period, as the pellet core and surface temperatures reach the furnace temperature. Seaton *et al.* (1983) were the first to highlight the problem of using chemical kinetics, and not taking heat transfer limitations into account. They showed that although chemical kinetic analysis of the results indicated the gasification reaction to be rate limiting, heat transfer calculations indicated heat transfer to the sample to be rate limiting, after the initial period of reaction. Recent work by Fortini and Fruehan (2005) confirms the importance of heat transfer in reaction of composite pellets reacted at 900-1280°C furnace temperatures. Fortini and Fruehan (2005) show that heat transfer control alone prevailed in composite pellets that contained highly reactive carbon in the form of wood charcoal, whilst chemical rate control prevailed in coal char containing pellets.

The only other laboratory scale study to consider heat transfer in reaction of iron ore and coal/carbon material mixtures is that of Huang and Lu (1993), and Sun and Lu (1996) who improved on the experimental set-up used by Huang and Lu (1993). A mixed bed of iron ore and coal, of 81% -75 µm and 88% -149 µm respectively, was reacted in a hollow cylindrical stainless steel crucible of 118 mm diameter and 150 mm height. The crucible was placed in a muffle furnace at 1200°C. Huang and Lu (1993) concluded from their results that heat transfer in the mixture was rate limiting. The

experimental set-up used by Huang and Lu (1993) was three-dimensional, or by approximation two-dimensional, although the intention was for it to give one-dimensional heating in the radial direction. The mathematical model, for this experimental set-up, was developed for a one-dimensional configuration. From the model predictions it was concluded that heat transfer within the material mixture is the rate-limiting step due to the endothermic reactions taking place, and the low thermal conductivity of the material mixture (Sun and Lu, 1992, 1993). Sun and Lu (1996) improved on the experimental set-up used by Huang and Lu (1993) by insulating the crucible sidewalls, and heating only the crucible bottom. This approach ensured that heat transfer was one-dimensional, or as close to it as experimentally possible. A mathematical model was developed to simulate the experiment (Sun and Lu, 1996, 1999a, 1999b). It was found that convection and radiation heat transfer within the mixed bed was negligible in comparison to conduction heat transfer, for furnace temperatures smaller than 1300°C. Heat flux to the sample, and within the sample was calculated in the model. From sensitivity analyses done on the model, it was concluded that conduction heat transfer within the material is rate-limiting to the reduction process.

A summary of the different studies in which apparent activation energies were calculated is shown in **Table 1** for coal containing samples and in **Table 2** for carbon containing samples. In the tables an opinion is given on which reaction systems can be considered to be reacted isothermally. In most of the studies apparent activation energies were calculated from the experimental data assuming isothermal reaction.

Depending on the amount of information obtained from the experimental measurements, the reaction extent for the individual reactions of reduction and gasification can be calculated. In absence of detailed information the reaction extent was expressed in terms of the sample mass loss measured, as a fraction of the maximum possible mass loss attainable. Kinetic parameters were then calculated in terms of the overall reaction extent. The resultant magnitude of the activation energy was then used to make conclusions as to the prevailing rate limiting step in the overall reaction sequence. As indicated by Seaton *et al.* (1983) this is questionable if non-isothermal conditions prevail because heat transfer may be the rate-limiting factor, but cannot be identified through chemical kinetic studies alone.

As seen from **Table 1 and 2** few studies were done with coal as reductant. Even when processes with coal as feed material are simulated, coal char is used rather than coal. This is done to avoid experimental difficulties in handling and analysing of coal product gases, and to simplify the reaction system so that conclusions can be made more easily from results. In most studies the contribution of coal volatiles to reduction has been ignored, and in some studies this contribution was inferred e.g. Mookherjee *et al.* (1986) and Haque *et al.* (1993) concluded reduction by volatiles based on the absence of an incubation period in the reduction kinetic plot for the initial reaction period when the

sample was still heating up to the furnace temperature. Dey *et al* (1993).viewed reacted composite pellet microstructures and concluded from these observations that reduction by volatiles took place along “favourable diffusional paths” and that volatiles release was too fast, at reaction temperatures above 1000°C, to contribute to reduction. Wang *et al.*(1997) showed that significant reduction by volatiles took place at temperatures above 700°C. The contribution of volatiles to reduction was calculated from mass loss information from isothermal reaction of a coal sample, an ore/alumina/coal layered sample and an ore/coal mixture, respectively. Sohn and Fruehan (2006a) followed a similar procedure to show that up to 56% reduction by volatiles occurred in a layered Fe_2O_3/coal sample heated from the top surface 1000°C. Sohn and Fruehan (2006b) showed that reduction by volatiles in a single layer of composite pellets was negligible, but in a three layer bed of pellets volatiles from the bottom pellet layer reduced the top pellet layer. The work by Wang *et al.* (1997) and Sohn and Fruehan (2006a, 2006b) were concentrated on composite pellets and not on the uni-directional heating of a packed bed of coal and ore. Therefore, the contribution of volatiles to reduction in a packed bed heated uni-directionally must be simulated in an experimental set-up that is representative of the material and heat transfer arrangement of the process under study to obtain quantified experimental evidence of volatile contribution to reduction for the particular process.

Table 1: Activation Energy calculated in Previous Studies on Ore Reduction with Coal

Authors	P/MB/FB[a]	*	FT[2] (°C)	Rate Equation[1]	Activation Energy (kJ/mol)	Particle Size (μm)
Mookherjee *et al*. (1986)	Ore column surrounded by coal	N	850 900 980 1050	$G(\alpha)=1-\frac{2}{3}\alpha-(1-\alpha)^{2/3}=kt$	Reduction: 156.2 Differential method: 130.7 at α=0.2, 152.1 at α=0.3, 144.7 at α=0.6 and 146.3 at α=0.70	-500 +250
Mookherjee *et al*. (1985a)	Ore column surrounded by coal	I	850 920 1000	$G(f)=1-\frac{2}{3}f-(1-f)^{2/3}=kt$	Reaction: 210	-500 +250
Mookherjee *et al*. (1985b)	Ore column surrounded by coal	N	1.7-2.4°C/min to 1100°C	$G(\alpha)=1-\frac{2}{3}\alpha-(1-\alpha)^{2/3}=kt$	Reduction from Coats & Redfern equation: 111.7	-500 +250
Haque *et al* (1993)	MB	N	900 950 1000 1050	$G(\alpha)=-ln(1-\alpha)=kt$	Reduction: Integral method: 159 Reduction: Differential method: 153 at α=0.20 and 160 at α=0.60	-2000 +1000
Haque *et al* (1993)	FB	N	900 950 1000	$G(\alpha)=-ln(1-\alpha)=kt$	Reduction: Integral method: 155 Reduction: Differential method: 152 at α=0.60 and 159 at α=0.50	Ore: -250 +180 Coal: -500 +353
Haque *et al* (1992a)	MB	N	950 1000 1050	None	Reduction: Differential method: 148-151.4 at α=0.6-0.9	-2000 +1000
Prakash and Ray (1990)	MB	I	800 900 1000	$G(\alpha)=1-\frac{2}{3}\alpha-(1-\alpha)^{2/3}=kt$	Reduction: 111.2 Reaction: 90.9	-6000 +3000
Prakash *et al*. (2000)	P	I	800 900 1000 1050	$G(\alpha)=-ln(1-\alpha)=kt$	Reduction: 49-50 (Pellet basicity=0.82); 47-52 (Pellet basicity=1.33)	-75 (Pellet ϕ = 10-12.5 mm)
Wang *et al*. (1998)	P	N	1050 1200 1250	$G(\alpha)=-ln(1-\alpha)=kt$	Reduction: Soft coal pellet: 82.61; Hard coal pellet: 68.95	(Pellet ϕ = 16-18 mm)
Reddy *et al*. (1991)	P	N	900 950 1000 1050 1100	$\frac{1}{C_{A0}(1.5-M)}ln\frac{M(1-X_A)}{(M-1.5X_A)}=kt$ $M=C_{A0}/C_{B0}$ C_{A0}=initial concentration Fe_2O_3 [g./mol] C_{B0}=initial concentration C [g./mol] X_A=fraction conversion of Fe_2O_3 to Fe	Reaction: Initial stage: 108.15; Latter stage: 93.16	-150 (Pellet ϕ = 14 mm)
Dey *et al*. (1993)	P	N	900 950 1000 1025 1050	None	Reaction: At different fraction reaction: 0.1: 35.0, 0.2: 30.3, 0.3: 40.5 and 30.3, 0.4: 44.2 and 30.3, 0.5: 44.2 and 30.3, 0.6: 44.2	-85 +53 (Pellet ϕ = 10 mm)
Shivarama-krishna *et al*. (1996)	P	N	950 1000 1050	$G(f)=-ln(1-f)=kt$	Reaction: Char: 138; Coal: 92	Ore: fine Coal: -500 +50 or –50 (Pellet ϕ = 10-12 mm)

*Isothermal = I; Non-isothermal = N

[1] α or f_r = reduction extent; f = reaction extent; f_c= gasification extent

[a] P = pellet; MB = mixed bed; FB = Fluidised bed

[2] FT = Furnace temperature

Table 2: Activation Energy calculated in Carbon Reduction Studies

Authors	P/MB [a]	*	Carbon Type	FT[2] (°C)	Rate Equation[1]	Activation Energy (kJ/mol)	#	Particle Size (μm)
Otsuka and Kunii (1969)	MB	I	Graphite	1050 1100 1150	None	At 20% R: 230 (C fine), 259 (C coarse), 272 (Both ore & C fine) At 60% R: 63 (both ore & C fine), 98 (fine ore, coarse C)	R	Ore mean size: fine = 20; coarse = 124 Graphite mean size: fine = 67; coarse = 190
Rao (1971)	MB	I	Amor-phous carbon	957 987 1007 1037 1087	$G(f) = ln(1.743 - f) = -kt + ln(1.743)$	301	O	Oxide: -4 Carbon: -49
Gosh and Tiwari (1970)	P	N	Lignite Coke	900 950 1000 1050 1100	None	At %R > 50%: 78	R	-250; (Pellet ϕ = 19 mm)
Srinivasan and Lahiri (1977)	P	N	Graphite	927 1022 1060 977	None	At 20% R: 418; At 60% R: 286; At 80% R: 56	R	-53; (Pellet ϕ = 9.7-12 mm)
Fruehan (1977)	MB, P	I	Coconut Charcoal, Coal Char, Metallurgi-cal Coke	900 950 1000 1050 1100 1200	$G(f_c) = -ln(1 - f_c) = k_c t$	$Fe_2O_3 \rightarrow$ FeO and FeO $\rightarrow$ Fe: 293-335	G	-75; (Pellet ϕ = 6-14 mm cylinder)
Abraham and Gosh (1979)	MB, OP-GP[4]	N	Electrode Graphite	880-1042	None	At %R < 20: MB: 305; MB (pressed): 296 At %R > 20: MB: 230; MB (pressed): 140 At 35-60%R: OP-GP: 314	G	Oxide: -49; Graphite: -75 +49; (Pellet ϕ = 15.2-17.2 mm, height = 2.8-6.6 mm)
Wright *et al.* (1981)	P (Iron Ore) in char	I	Char	900 950 1000 1075 1150 1200	$G(\alpha) = -ln(1-\alpha) = kt$	290-335	R	(Ore Pellet ϕ = 12 mm) Char: -8 +1 mm
Seaton *et al.* (1983)	P	N	Coal Char	900 1000 1100 1150	$G(\alpha) = ln(1 - 0.98f) = -kt$ $G(\alpha) = ln(1 - 1.037f) = -kt$	Heamatite: 126, 239 Magnetite: 159	O	Ore: ? Char: -49 (Pellet ϕ = 14 mm)
Roman-Moguel and Brimacombe (1988)	MB	N	Coal Char	800 850 900 950	Gasification: $G(f_c) = -ln(1 - f_c) = k_c t$ Reduction: $G(f_r) = 1 - (1 - f_r)^{1/3} = k_r t$	Gasification: Coal char: 224; Lignite: 264 Reduction: 116.4	R & G	Ore: -420 +300 Coal char: -210 +150
Mookherjee *et al.* (1985a)	Ore column in char	I	Coal Char	850 920 1000	$G(f) = 1 - \frac{2}{3}f - (1-f)^{2/3} = kt$	195.8; 168.8 (5% Na_2CO_3 added to char) Differential: 188.1 at f=0.3; 144.2 at f=0.4 Na_2CO_3 added to char: 179.9 at f=0.3; 152.0 at f=0.4	O	-500 +250
Mookherjee *et al.* (1985b)	MB	N	Coal Char	10°C/min; 20°C/min to 1100°C	$G(f) = -ln(1 - f) = kt$	Last segment of Non-isothermal kinetic plots: Coats-Redfern equation = 99; Dixit-Ray equation = 114	O	-90 +63
Mookherjee *et al.* (1985b)	Ore column in char	N	Coal Char	10°C/min to 1100°C	None	119	O	-500 +250
Mookherjee *et al.* (1986)	Ore column in char	I	Coal Char	850 900 950 1000	$G(\alpha) = 1 - \frac{2}{3}\alpha - (1-\alpha)^{2/3} = kt$ $G(f_c) = 1 - \frac{2}{3}f_c - (1-f_c)^{2/3} = kt$	Reduction: 168.4 Gasification: 176.6	R & G	-500 +250

Authors	P/MB [a]	*	Carbon Type	FT[2] (°C)	Rate Equation[1]	Activation Energy (kJ/mol)	#	Particle Size (μm)
Ajersch (1987)	P	N	Electrode Graphite	837 1127 1027	None	$Fe_2O_3 \rightarrow$ FeO: 169 (initial), 182 (steady) FeO → Fe: 647	R	Oxide: -57 +44; Graphite: -105 +74; (Pellet ϕ = 10 mm = height)
Nasr *et al.* (1994)	P	N	Coke	950 1000 1050 1100	$ln(A-R) = -kt + ln(A)$ $R = AC_u + B$ R = %Reduction; C_u = %Carbon utilisation; A, B are constants	5% Coke in mix: 231; 10% Coke in mix : 179; 15% Coke in mix: 159; 20% Coke in mix: 123	R	-75 (Pellet ϕ = 7.5 mm, height = 10 mm)

*Isothermal = I; Non-isothermal = N; [a] P = pellet; MB = mixed bed; [4] OP-GP = Oxide pellet – graphite powder, 1.6 cm apart
[1] α or f_r = reduction extent; f = reaction extent; f_c= gasification extent. %R=%Reduction; [#] Reaction measured in study: R = reduction; G = Gasification; O = Overall reaction; N = None

Studies on coal devolatilisation as applicable to ore reduction are limited. Sampaio *et al.* (1992) experimentally simulated coal devolatiliation of 3-9 mm particles in slag at 1325, 1435, 1520°C at heating rates of 5640, 7020, 10140°C/min applicable to bath smelting processes, and Patisson *et al.* (2000) simulated devolatilisation of 10 mm coal particles in a rotary kiln at 8, 14, 30 °C/min up to 850°C.

The heating rates used by Patisson *et al.* (2000) are rather low but this work does give valuable information on the expected devolatilisation products: C_2H_4, C_2H_6, C_2H_2, CO_2, CO, H_2, H_2O and tar. Increased heating rates resulted in more light gases and less tar being formed. The studies on the mechanism and reaction sequences in coal pyrolysis indicate the rate and extent of coal devolatilisation to be dependent on the heating rate of the coal (Tomeczek and Kowol, 1991; Goyal and Rehmat, 1993; Devanathan and Sexena, 1987; Jones and Schmid, 1964; Arendt and van Heek, 1981; Peters and Bertling, 1965; Jüntgen and van Heek, 1979). At high heating rates secondary reactions occur, in which coal tar (forming in the devolatilisation process) is further cracked to simple components such as H_2, char and gas (Devanathan and Sexena, 1987). Generally, for a coal, an increased heating rate results in a higher devolatilisation temperature, and an extended temperature range of devolatilisation (Pattison *et al.*, 2000). Coal heated to high temperatures at high heating rates can evolve more volatile matter than that found in the proximate analysis (Desypris *et al*., 1982). Primary devolatilisation of coal starts at 300-400°C, and continues at higher temperatures up to 1000°C for high heating rates (Stubington and Sumaryonon, 1984; Arendt and van Heek, 1981).

Information on the extent of carburisation of the iron formed in the solid state reduction product at the heap surface is important because the final product aim is making crude steel. If the product from the solid state reduction zone is high in carbon, refining must be done in the rest of the process. Few studies were done to investigate carburisation of iron by coal in mixed ore-coal reaction. Haque *et al.* (1992b, 1993) measured carburisation of iron in reaction of coal-ore packed beds and found increased carbon deposition at lower temperatures. Haque *et al.* (1992b, 1993) explain this to be the result of

slow devolatilisation and slow dissociation of volatiles at low temperatures, enhancing formation of deposited carbon. Formation of combined carbon is enhanced by increased reaction time and temperature. In the case of char as reductant only small amounts of free carbon is formed, and according to Haque *et al.* (1992b, 1993) this carbon deposition took place on sample cooling. The combined carbon content of DRI, when char was used as reductant, is similar to that formed when coal was used as reductant. Additions of Na_2CO_3 or $CaCO_3$ resulted in increased combined carbon contents. Haque *et al.* (1992b, 1993) ascribed this to early formation of iron in the presence of the carbonates, so increasing the contact time between carbon and iron for diffusion of carbon into iron.

Towhidi and Szekely (1983) performed reduction experiments on Fe_2O_3 pellets in CO-H_2-N_2 gas mixtures at 600-1234°C and found that the maximum rate of carbon deposition occurred at 500-600°C. Carbon deposition only occurred at temperatures below 900°C and formed a layer of carbon on the pellet surface that prevented access of reducing gas to the pellet, resulting in decreased reduction rates. The gas mixtures used in experiments varied from CO and H_2, to mixtures of CO and H_2 of 25%CO-75%H_2, 50%CO-50%H_2 and 75%CO-25%H_2. The maximum rate of carbon deposition was observed in a 75%CO-25%H_2 gas mixture. At constant partial pressure of CO, carbon deposition was enhanced by H_2 and hindered by N_2. Deposited carbon was elemental carbon, not cementite. Carbon deposition is not only dependent on thermodynamics as it was found that carbon deposition does not take place to a significant extent in the initial stages of reduction, but once iron had formed from reduction, the iron served as a catalyst for carbon deposition.

The catalytic effect of iron on CO decomposition means that the pore surface area of the iron formed in the reduction process directly influenced the carbon deposition rate (Turkdogan and Vinters, 1974). The product iron surface area formed in reduction of hematite in turn depends on the pore surface area of the source material as shown by Turkdogan and Vinters (1972); a small iron oxide surface area (porosity) results in a small iron surface area. Turkdogan and Vinters (1972) also determined that the coarseness of the iron pore structure formed from hematite reduction increases with increased reduction temperatures, and the iron pore surface area decreases. Also, a more coarse iron pore structure is formed from reduction by CO than that formed by H_2 reduction.

1.3. Indicators for Heat Transfer Control

Pistorius (2005) identified heat transfer control of three different types: (1) thermodynamically constrained processes such as calcination of limestone which takes place at a specific temperature where increased heat input results in increased reaction rate at the specific reaction temperature, (2) processes in which the process temperature is limited by the slag liquidus temperature so that increased heat input results in increased reaction rate, but process temperatures remain similar to that at lower heat input as is the case in ferromanganese and ferrochromium production, (3) reaction of

ore-carbon/coal systems in which there is a band of reaction temperatures in which the process can function, given no bulk melting of reactants and products takes place. As shown by Pistorius (2005) mixed control between heat transfer control and chemical reaction control can prevail in ore-carbon/coal reaction systems, and heat transfer control can be in the form of radiation heat transfer control, that is heat transfer from the heat source to the heated surface is controlling, or heat transfer control can be in the form of conduction heat transfer (where heat transfer from the sample surface to the sample interior is limiting).

The main indicator for heat transfer control is the presence of a persistent temperature differential between the heat source and the heated surface. This was shown by Venkateswaran and Brimacombe (1977) to be the case in the SL/RN direct reduction kiln process. The authors developed a model for the process and compared the model outputs with solids bed temperature measurements from a pilot SL/RN kiln of 35 m length and 2.1 m ID. The temperature differential between the solids bed and the gas varied from a maximum of 597°C closest to the charge end, in the reduction zone of the kiln, to a minimum of 165°C towards the discharge end of the kiln. At the same physical positions in the kiln, the temperature differential between the solids bed and the kiln wall varied from 247°C to 41°C. Venkateswaran and Brimacombe (1977) conclude that heat transfer control prevails in the reduction zone of the kiln because the air profile in the kiln is an important variable, and that high energy requirement for the gasification reaction explains heat transfer control in the reduction zone. Heat transfer control in the SL/RN process is also indicated by the effect of more reactive reductant on the bed temperature. This is shown in graphical format by Cunningham and Stephenson (1980): for lignite as reductant the bed temperature is 900°C, increasing to 1000°C for gas-flame coal, and a further increase to 1140°C for coke breeze as reductant. In the work presented here the sample is heated uni-directionally from the sample surface to test the effect of heat transfer control within the material bed. Therefore, in the experimental work presented here a significant temperature differential, at least 100°C, between the sample surface and the heat source is expected.

Besides the observation of a persistent temperature differential between the heat source and the heated surface, the second indication of heat transfer control in a reaction system is that increased reaction rates result from increased heat transfer to the reacting material. The latter statement sounds obvious for an endothermic reaction system but can be better explained from the work of Seaton *et al*. (1983) in which the reaction of char-hematite composite pellets almost ceases for reaction at 900°C when the pellet surface and centre temperatures levelled off with the onset of the gasification reaction. For reaction of the pellets at 1000°C and 1100°C furnace temperatures, instead, the similar eventual levelling off of pellet surface and centre temperatures is seen, but the reaction extent was much larger before reactions ceased. Therefore, as pointed out by Seaton *et al*. (1983), not enough heat is transferred to the pellet at 900°C to overcome the heat demand of the gasification reaction at this

temperature, whilst heat supply to the pellet at 1000°C and 1100°C furnace temperature was higher to at least enable significant gasification reaction progress to supply CO for the reduction of FeO. The latter observation does not mean the absence of heat transfer control at 1000°C and 1100°C furnace temperatures, only that the effect of heat transfer control was more pronounced at 900°C.

Another indicator of heat transfer control is the observation of apparent activation energy values which are much lower than that for chemical reaction control. In some studies a possible explanation put forward for the lower apparent activation energy was catalysis of the gasification reaction, Seaton *et al*. (1983), Abraham and Gosh (1979). The other explanation often put forward is mixed control because the activation energy is close to half that reported by Walker *et al*. (1959) of 360 kJ/mol for chemical reaction control.

1.4. Chemical Reaction Rates

1.4.1. Reduction

Usually the aim of rate chemical studies of reduction/gasification is to determine the intrinsic reaction rate for a particular material. To measure the intrinsic reduction/gasification rate the experiment must be set up in such a way that effects of film mass transfer and diffusion are eliminated. Reacting small samples at low temperatures and under sufficient gas flow rates ensure that only the chemical reaction rate is measured. This information provides the absolute maximum rate at which reduction/gasification can take place. However, rates in industrial processes are usually not under chemical reaction control only, since high reaction temperatures are employed. Relevant reduction rate studies are summarised in **Table 3**. Comparison of the rate data from these studies is shown in graphical format in Coetsee *et al*. (2002).

Table 3: Studies on Reduction Rates

Authors	Year	Activation Energy (J/mol)	Reaction Step*	Reduction Temperature (°C)	Gas	Start Material	Particle Diameter/ Thickness (mm)	A/N/ D/C/ S/PB
McKewan	1960	64 015	W/F	600-1050	H_2	Ore fines	5-18; 6-25 (Hard Taconite)	P
McKewan	1960	62 342	M/F	400-550	H_2	Ore fines	5-18; 6-25 (Hard Taconite)	P
McKewan	1961	56 902	M/F	400-500	H_2-H_2O-N_2	Reagent Grade Fe_2O_3	9	P
McKewan	1962a	57 739	H/F	700-1000	H_2-H_2O-N_2	Reagent Grade Fe_2O_3	9	P
McKewan	1962b	56 484	M/F	350-500	H_2	Reagent Grade Fe_2O_3	9	P
Trushenski *et al.*	1974	99 998 64 434 [105 397?]	H/M M/W	750, 775, 800	CO-CO_2	Pure Fe_2O_3 Powder	13.5	P
Trushenski *et al.*	1974	69 036 78 241 116 131	H/M M/W W/F	750, 775, 800	CO	Pure Fe_2O_3 Powder	13.5	P
Turkdogan & Vinters	1972	191 409	W/F	600-1100	H_2	Hematite Ore	0.4-3.6	A
Turkdogan & Vinters	1972	125 614	W/F	700-1200	CO-CO_2	Hematite Ore	0.4-3.6	A
Turkdogan & Vinters	1972	137 439	W/F	800, 1050, 1200	CO-CO_2	Oxidised Fe Strip	1 x (4-11 cm^2)	S
Nabi & Lu	1968	92 048	H/M	811-1011	H_2-H_2O	Hematite Ore	9.3 x 27 length	C
Quets *et al.*	1960	61 505	M/F	400-590	H_2-N_2	Reagent Grade Fe_2O_3 & Fe Strip	15.6 (C) 20 x 15 x 0.1 (S)	C, S
Quets *et al.*	1960	13 389	M/W	590-1000	H_2.N_2	Reagent Grade Fe_2O_3 & Fe Strip	15.6 (C) 20 x 15 x 0.1 (S)	C, S
El-Geassy *et al.*	1977	53 555 (Dense) 21 506 (Porous)	H/F	800-1100	H_2	Chemically Pure Fe_2O_3	Dense: 9.8 x 11.1 height Porous: 10.8 x 12.2 height	C
El-Geassy *et al.*	1977	31 589 (Dense) 9 540 (Porous)	H/F	800-1100	CO	Chemically Pure Fe_2O_3	Dense: 9.8 x 11.1 height Porous: 10.8 x 12.2 height	C
Murayama *et al.*	1978	79 161 120 499 125 143	H/M M/W W/F	800-1050	CO-CO_2	Pyrite Cinder	10	P
El-Rahaiby & Rao	1979	71 550	W/F	238-417	H_2	Fe Strip	0.0508 x (2.40-5.28 cm^2)	S
Al-Kahtany & Rao	1980	77 739	M/F	234-620	H_2	Fe Strip	0.089 x (1.12-9.88 cm^2)	S
Sun and Lu	1999b	65 689 69 454 73 638	M/W W/F M/F	1200	CO (Coal)	Fe_3O_4	Fines	PB
Sun and Lu	1999b	61 505 63 597 68 618	M/W W/F M/F	1200	H_2 (Coal)	Fe_3O_4	Fines	PB
Rao & Moinpour	1983	65 325	H/F	245-482	H_2	Fe Strip	0.136x (6.40-6.56 cm^2)	S
Towhidi and Szekely	1981	52 300	H/M	600-1234	CO	Fe_2O_3	4-20	P
Towhidi and Szekely	1981	60 668	H/M	600-1234	H_2	Fe_2O_3	4-20	P

Authors	Year	Activation Energy (J/mol)	Reaction Step*	Reduction Temperature (°C)	Gas	Start Material	Particle Diameter/ Thickness (mm)	A/N/ D/C/ S/PB
Warner	1964	63 597	W/F	650-950	H_2	Fe_2O_3	10 x 10 height	C
Meraikib & Friedrichs	1987	63 100	H/F	800-1000	CO	Hematite Ore	13	P
Meraikib & Friedrichs	1987	51 700	H/F	750-1000	H_2	Hematite Ore	13	P
Tsay *et al.*	1976	92 048 [Nabi & Lu] 71 128 63 579 [Warner]	H/M M/W W/F	800, 850, 900	H_2	Fe_2O_3	28.6 x 10 height	P
Tsay *et al.*	1976	113 805 73 638 69 454	H/M M/W W/F	800, 850, 900	CO	Fe_2O_3	28.6 x 10 height	P

* Pellet (P) or Particle (A) or Disk (D), or Cylinder (C), Packed Bed of Coal and Oxide (PB), Strip (S)
* Fe_2O_3=H; Fe_3O_4=M; FeO=W; Fe=F

1.4.2. Gasification

Gasification of carbon occurs via a surface reaction on the carbon pore surface. Therefore, as in the case of iron oxide reduction with CO, experimental measurement of fundamental kinetics requires prevention of diffusion control, by using small particles. The pore surface area and pore size distribution are different for different types of carbon. Also, as the carbon is gasified the pore structure changes: the pores increase in size when carbon is carried away in the gas phase as CO.

Global kinetic parameters were determined in most of the gasification studies, but some authors determined the kinetic parameters for the elementary steps in the gasification process, as presented in the Langmuir-Hinshelwood (LH) expression. The latter approach involves the reaction of carbon under different CO_2-CO gas mixtures, at different temperatures, whilst the former may be calculated from gasification experiments under CO_2 gas only. As it is well known from experimental evidence that the gasification rate is retarded by CO and H_2 in the reactant gas it would seem appropriate to measure gasification rates in the presence of these retarding gases, since they will be present in significant quantities in metallurgical processes.

However, there still remains much uncertainty as to the applicability of the LH expression, and the meaning of the constants in the expression. Wu *et al*. (1988) questioned the interpretation of the constants in the LH expression and Bandyopadhyay and Ghosh (1996) questioned the applicability of the expression for CO-CO_2 gases containing large amounts of CO.

The LH equation is:

$$rate = \frac{K_1 P_{CO_2}}{1 + K_2 P_{CO} + K_3 P_{CO_2}} \qquad (1)$$

The widely accepted mechanism as represented in the LH expression is that proposed by Reif (1952):

$$CO_2 \underset{k_2}{\overset{k_1}{\Leftrightarrow}} (O) + CO \qquad (2)$$

$$C + (O) \xrightarrow{k_3} CO \qquad (3)$$

$K_1 = k_1; K_2 = k_2 / k_3; K_3 = k_1 / k_3$

(O) = carbon-oxygen complex formed by adsorption of oxygen onto the carbon surface

As discussed by Von Fredersdorff and Elliott (1963), the LH expression can be simplified for extreme reaction conditions of temperature and partial pressures of CO and CO_2, for total pressures up to 1 atm. If gasification occurs at low temperature and high P_{CO_2}, the P_{CO} will be low and the simplified LH expression will be zero order with respect to P_{CO_2} as $K_2 P_{CO} << 1$ and $K_3 P_{CO_2} >> 1$. Most of the active carbon sites are then filled by adsorped oxygen and the gasification rate is that of the gasification step, reaction (3), and the activation energy, E_{k_3}. Dutta *et al*. (1977) found that the gasification rate is independent of P_{CO_2} at CO_2 pressures in excess of 15 atm., and therefore zero order with respect to P_{CO_2}.

At low P_{CO_2} and low temperatures, when P_{CO} is low, the LH expression simplifies to express the rate of the oxygen adsorption reaction step, reaction (2), as $K_2 P_{CO} << 1$ and $K_3 P_{CO_2} << 1$. The reaction order with respect to P_{CO_2} is then one. This is also the case when gasification takes place at high temperature and P_{CO_2}, because the K_2 and K_3 become small under these conditions. That is, the gasification reaction rate constant (k_3) is large compared to the oxygen adsorption and desorption reaction rate constants, k_1 and k_2 so that most of the active carbon sites are free carbon sites. The gasification rate expressed is that of the oxygen adsorption rate, reaction (2) forward, and the activation energy is E_{k_1}.

The extreme reaction conditions that allow simplification of the LH equation are usually absent in ore-carbon reduction. Then the reaction order with respect to P_{CO_2} falls between one and zero. As indicated by Von Fredersdorff and Elliott (1963), the LH expression does not allow for zero gasification rates at equilibrium conditions when high P_{CO} prevails at ore-carbon reduction temperatures. Rao and Jalan (1972) show that incorporation of the reverse reaction (3) results in a modified LH expression that does eliminate the above problem. Reaction (3) (reverse) was not taken into account in the past as the argument was that carbon transfer from gas to solid carbon would occur if this reaction takes place, and this was not seen in previous studies, Ergun (1956). The contrary was concluded by Kapteijn *et al*. (1994).

The gasification mechanism under water vapour may be considered to be analogous to that of gasification under CO_2:

$$H_2O \underset{k_2}{\overset{k_1}{\Leftrightarrow}} (O) + H_2 \quad (4)$$

$$C + (O) \xrightarrow{k_3} CO \quad (5)$$

$K_1 = k_1; K_2 = k_2 / k_3; K_3 = k_1 / k_3$
(O) = carbon-oxygen complex formed by adsorption of oxygen onto the carbon surface

The LH equation for steam gasification of carbon:

$$rate = \frac{K_1 P_{H_2O}}{1 + K_2 P_{H_2} + K_3 P_{H_2O}} \quad (6)$$

In most instances the gasification rate is determined under CO_2 (or H_2O) gas only, and the apparent activation energy is calculated from the first order reaction rate expression. In some instances the reaction order with respect to P_{CO_2} is checked, but in most cases it is assumed. Also, the initial reaction rates are used so that the carbon pore surface area used in rate calculations can then be assumed to be the same as that measured in the unreacted carbon. The rates are compared in units of per time here for easy comparison as the internal pore surface area has not been measured in all the studies. The use of small particles is very important in gasification rate measurements as the internal surface area is large so that diffusion control can easily set in when large particles are used. Turkdogan *et al*. (1968) determined that the carbon particles should be smaller than 6 mm at 900°C and 2 mm at 1100°C to ensure reaction control under CO_2.

In **Fig. 2** the reaction rates from various studies, at 1 atm. total pressure CO_2, are shown. Where points are indicated in the graphs these points were calculated from individual data points in the reported study, whilst lines without points indicate extrapolation of data measured at low temperatures or a rate expression determined by the authors and then only converted to the required units for this study. Where a data series consists of both points and a line, the line represents a linear fit determined in this study, and the kinetic parameters from this straight line may not be exactly that reported in the particular study.

It is seen that the reaction rates range from lowest rates for unreactive graphite, to petroleum coke, coal char and most reactive coconut charcoal. The activation energies range from 164 kJ/mol for Pitch coke by Kühl *et. al.*(1992) to 325 kJ/mol for Carbon Black by Rao and Jalan (1972). The reaction rates measured by Kühl *et al*. (1992) for different coke samples are higher than the rest. This may be due to the rates being measured at 40% carbon reaction, when the pore surface area should be close to its maximum value, Wu *et al*. (1988).

Fig. 2: Initial Gasification Rates under CO_2

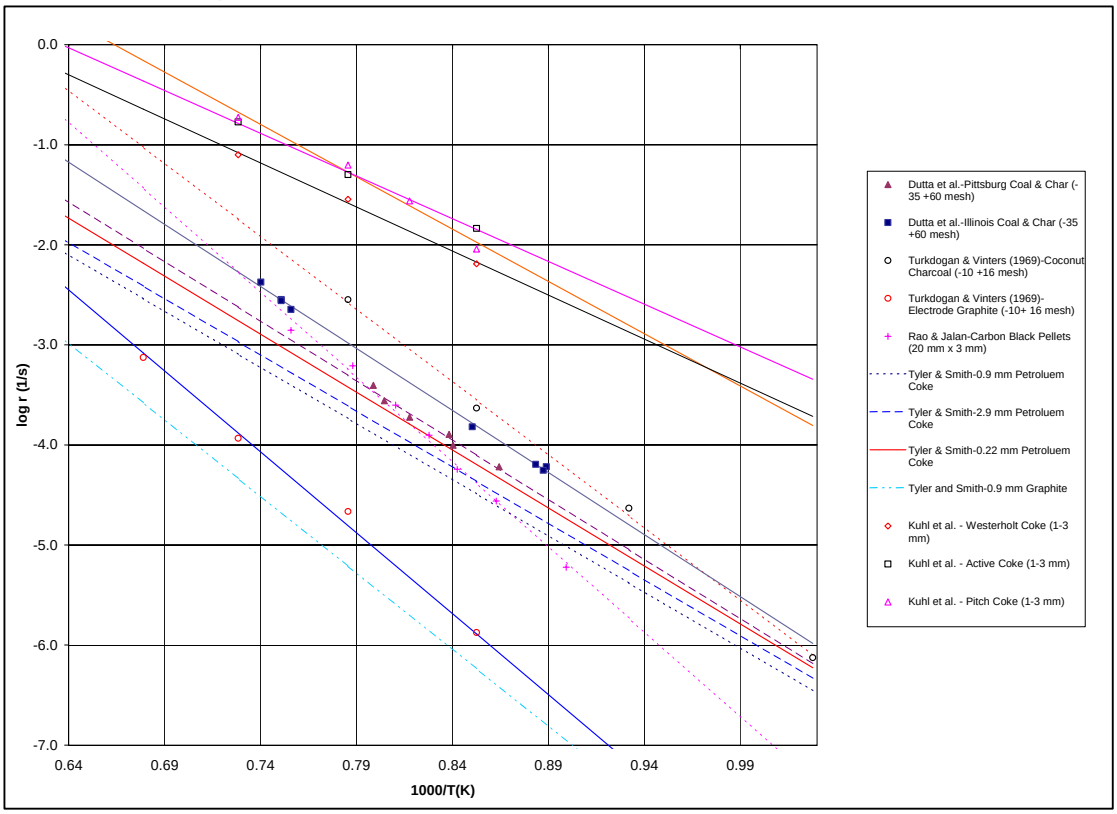

A limited number of studies have been done on steam gasification of carbon. **Fig. 3** shows some of the initial reaction rates from these studies under 1 atm. H_2O. The values reported for Johnstone *et al.* (1952) and Blackwood and McGrory (1958) were calculated from the LH-expression parameters determined in those studies. Kayembe and Pulsifer (1976) calculated an activation energy of 254 kJ/mol for coal char gasification under steam. This value is much higher than that determined in the other studies done by Pilcher *et al*. (1955), Johnstone *et al*. (1952) and Kühl *et al*. (1992) ranging from 120-177 kJ/mol. The gasification rates measured by Kühl *et al*. (1992) for different coke types are also higher than that measured in the other studies, but this may be due to the rates being measured at 40% reaction, when the carbon surface area is close or at its maximum, Wu *et al.* (1988).

Fig. 3: Initial Gasification Rates under H_2O

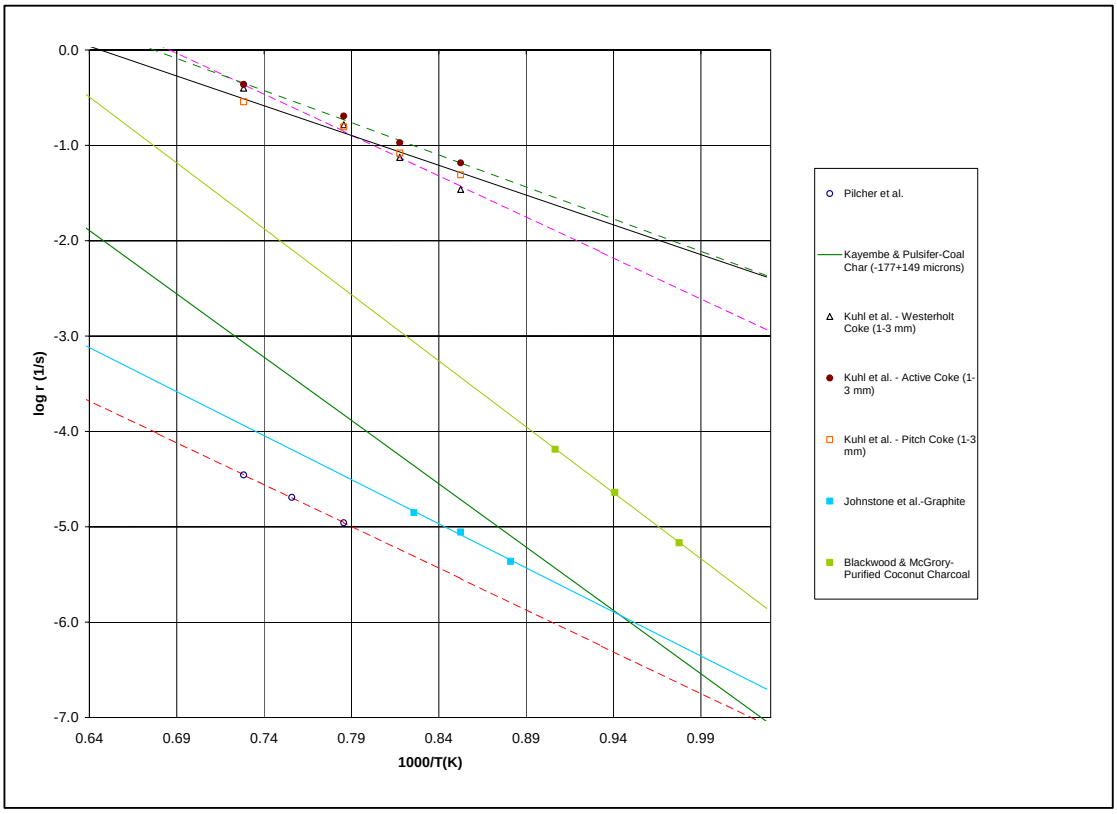

1.5. Conclusion

Chemical reaction rates of reduction and gasification indicates the maximum possible process production rates for mixed bed systems, but do not necessarily provide realistic process production rate predictions because the real process in usually not under chemical reaction control. Apparent activation energy values calculated from experiments on composite pellets and mixed bed materials can not be used alone to make conclusions on heat transfer control, as pointed out by Seaton *et al*. (1983). As pointed out by Vankateswaran and Brimacombe (1977) a lot of work is required to obtain all the necessary detailed fundamental information to describe the process progress in a mixed bed system so that an empirical approach to reaction rate measurements is more effective. Therefore, the primary aim of the work presented here is to construct a realistic simulation experiment to quantify radiation heat transfer from measurement of temperature and reaction extent as functions of reaction time and position within the sample material. These results will show the importance of heat transfer in the IFCON® process. Secondary aims of this work are to show the effects of layer thickness, coal volatiles, phase chemistry and particle size in this reaction system. The information gained from such an experiment should provide enough information to use in validation of mathematical models that can then be used for process design and testing process sensitivities.